# Luminescence properties of layered perovskites activated by Eu$^{3+}$ ions

Kenji Toda [a], Yutaka Kameo [b], Masatoshi Ohta [b], Mineo Sato [b]

[a] *Department of Active Material Chemistry, Graduate School of Science and Technology, Niigata University, 8050 Ikarashi 2-nocho, Niigata-shi 950-21, Japan*

[b] *Department of Chemistry and Chemical Engineering Faculty of Engineering, Niigata University, 8050 Ikarashi 2-nocho, Niigata-shi 950-21, Japan*

Received 9 June 1994; in final form 25 August 1994

## Abstract

Dependence of emission intensity on Eu$^{3+}$ concentration in Na$_2$Gd$_{2(1-x)}$Eu$_{2x}$Ti$_3$O$_{10}$ with a triple perovskite layer and NaGd$_{1-x}$Eu$_x$TiO$_4$ with a single perovskite layer was studied. Critical values for concentration quenching are $x=0.40$ for Na$_2$Gd$_{2(1-x)}$Eu$_{2x}$Ti$_3$O$_{10}$ and $x=0.25$ for NaGd$_{1-x}$Eu$_x$TiO$_4$. The difference in the critical concentration between both compounds is discussed in terms of their crystal structures determined by the powder X-ray diffraction patterns using the Rietveld method. The concentration quenching found in these compounds can be explained by means of a percolation model with nearly two-dimensional interactions between Eu$^{3+}$ sites in the host lattice.

*Keywords:* Luminescence; Concentration quenching; Crystal structure; Rietveld analysis; Layered perovskite

## 1. Introduction

Many compounds containing rare earth ions are very useful for phosphors and laser materials because rare earth ions can become an efficient luminescence centre [1]. The emission is often quenched by doping rare earth ions over a critical concentration [2,3]. This phenomenon is called 'concentration quenching'. It is well known that the interaction between rare earth ions results in concentration quenching, but there are a number of unclarified discussions regarding the nature of the interaction. Although the concentration quenching is strongly dependent on the structural dimensionality of the host material, investigations on the luminescence properties of low-dimensional compounds are rather fewer than those on three-dimensional compounds [4–6]. In addition, these studies have not been carried out systematically.

In this paper, we have studied the relationship between the structural arrangement of rare earth ions and the concentration quenching of luminescence in layered perovskite compounds of Na$_2$Gd$_{2x}$Eu$_{2(1-x)}$Ti$_3$O$_{10}$ with a triple perovskite layer and NaGd$_x$Eu$_{1-x}$TiO$_4$ with a single perovskite layer. The crystal structures of these compounds remain still unknown although prototype structure models are pre-

sumed [7,8]. Therefore, the crystal structures of both compounds were determined by the Rietveld analysis for powder X-ray diffraction (XRD) data. The difference in the critical concentration for the concentration quenching observed in both compounds is discussed on the basis of the determined crystal structure.

## 2. Experimental details

Na$_2$Gd$_{2x}$Eu$_{2(1-x)}$Ti$_3$O$_{10}$ and NaGd$_x$Eu$_{1-x}$TiO$_4$ were prepared by a solid state reaction. The starting materials were mixtures of Na$_2$CO$_3$, Gd$_2$O$_3$, Eu$_2$O$_3$ and TiO$_2$ powders. An excess amount of Na$_2$CO$_3$ (30 mol.%) was added to compensate for the loss due to the evaporation of the sodium component during the firing. The mixture was heated at 500–700 °C for 12 h and subsequently fired at 1000–1100 °C for 6 h in air. After the reaction, the product was washed with distilled water and dried at 100 °C for 24 h.

Powder XRD patterns were recorded on a Rigaku RAD-rA diffractometer, using Cu K$\alpha$ radiation which was monochromatized by a curved crystal of graphite. The data were collected on thoroughly ground powders by a step-scanning mode in the $2\theta$ range 5°–100° with a step width of 0.02° and a step time of 4 s. The

indexing of the powder XRD pattern for these compounds was examined with the aid of the computer program CELL [9]. Data analysis for the structural refinement was carried out by the Rietveld method, using the RIETAN profile refinement program [10] on an ACOS2010 computer at Niigata University.

Phase purity of these compounds was examined by the energy-dispersive X-ray (EDX) method using an electron microscope (ABT EM002B) equipped with an EDX analyser. Excitation and emission spectra were measured on a powder sample using a Shimadzu RF-5500 spectrophotofluorometer.

## 3. Results and discussion

The space group of $Na_2Ln_2Ti_3O_{10}$ (Ln = rare earths) has not been found. Gondrand and Joubert [7] reported the synthesis of a series of $Na_2Ln_2Ti_3O_{10}$ compounds (Ln = La, Nd, Eu, Gd). From the electron diffraction analysis, they suggested that $Na_2Gd_2Ti_3O_{10}$ crystallizes in an orthorhombic system with $a \approx b \approx 0.770$ nm and $c \approx 2.84$ nm. They also pointed out that the structure of these compounds is analogous to that of the Ruddlesden–Popper-type compound, $Sr_4Ti_3O_{10}$, with a triple perovskite layer because the $a$ and $b$ lattice parameters were nearly equal to values twice as large as those of the Ruddlesden-Popper compound with $I4/mmm$ space group. We also observed weak electron diffraction spots corresponding to the doubling of $a$ and $b$ lattice parameters for $Na_2Eu_2Ti_3O_{10}$. According to the group theoretical analysis of space groups by Hatch et al. [11], we tried to determine the possible space group for $Na_2Eu_2Ti_3O_{10}$. However, the Rietveld analysis using the several space groups expected from the group theory gave no reasonable solution with physically meaningful structural parameters. This type of superstructure of $Na_2Eu_2Ti_3O_{10}$ is probably related to an only slight displacement of oxygen atoms, as observed in Ba-NdMnO$_4$ [12]. Therefore, we carried out the Rietveld analysis based on the space group $I4/mmm$ ($Z = 2$). It should be noted that the results in the present structural determination express an averaged structure for $Na_2Eu_2Ti_3O_{10}$.

In the earlier study [13], the space group of $NaLnTiO_4$ (Ln = rare earths) was reported to be $P4mm$ with a tetragonal symmetry, although the refinement of crystal structure was unsuccessful. Linares and Blanchard [14] pointed out that the symmetry of the lanthanide site in the $NaLnTiO_4$ is lower than $C_{4v}$ because the number of lines observed in the emission spectra of NaLn-TiO$_4$:Eu is much more than those expected from usually assumed symmetry $C_{4v}$. In addition, the XRD patterns exhibited weak extra reflections which could not be explained according to the tetragonal cell with $P4mm$ space group. These results clearly indicate that

$NaEuTiO_4$ has a lower symmetry than $P4mm$. Therefore, we re-examined the indexing of the XRD patterns of $NaEuTiO_4$ by means of the CELL program. The reflection conditions found are $k = 2n$ for $0kl$ and $0k0$ reflections and $l = 2n$ for $h0l$ and $00l$ reflections on the basis of an orthorhombic symmetry. These conditions lead to $Pbcm$ and $Pbc2_1$ space groups. In this study, we adopted the $Pbcm$ space group, with higher symmetry than $Pbc2_1$, because some of the standard deviations for structural parameters became fairly large (sometimes of the order of about $10^{-2}$) in the case of the $Pbc2_1$ space group for the Rietveld refinement. $NaGdTiO_4$ was also isomorphous with $NaEuTiO_4$.

The results of the pattern fitting for both compounds are shown in Figs. 1 and 2. The crystallographic data finally obtained from the Rietveld refinement are listed in Tables 1 and 2. The structural models for $Na_2Eu_2Ti_3O_{10}$ and $NaEuTiO_4$ are illustrated in Figs. 3 and 4 respectively. These compounds exhibit an ordering of the cations in the form [–Eu–Eu–Na–Na–]. In both compounds, the charge imbalance between Na$^+$ and Eu$^{3+}$ ions both located in the interlayer is compensated by a displacement of the Ti$^{4+}$ ions from the position of a regular octahedral centre toward the Na$^+$ ions. Such a distortion of TiO$_6$ octahedra in their compounds is contrasted with that of the Ruddlesden–Popper phase, $Sr_3Ti_2O_7$, which has an almost regular TiO$_6$ octahedral structure [15]. Blasse and Van Den Heuvel suggested from the IR and Raman spectra of $NaLnTiO_4$ (Ln = La, Gd and Y) that the position of Ti atom in the TiO$_6$ octahedra is shifted from a regular central position [13]. Our structure refinement results obtained here strongly support their prediction. The Eu$^{3+}$ ions occupy only one crystallographic site and form a quasi-two-dimensional plane consisting of a double layer perpendicular to the $c$ axis in $Na_2Eu_2Ti_3O_{10}$ and the $a$ axis in $NaEuTiO_4$. The shortest Eu$^{3+}$–Eu$^{3+}$ distances (ca. 0.38 nm in both compounds) within the quasi-two-dimensional plane are much shorter than those between the adjacent two planes (ca. 0.98 nm in $Na_2Eu_2Ti_3O_{10}$ and ca. 1.25 nm in $NaEuTiO_4$). The shortest Eu$^{3+}$–Eu$^{3+}$ distances are about the same in both compounds. Therefore, these layered perovskite compounds can be a suitable system to investigate two-dimensional energy transfer among doped Eu$^{3+}$ ions.

Fig. 5 shows the emission spectra for $Na_2Gd_{2(1-x)}Eu_{2x}Ti_3O_{10}$ and $NaGd_{1-x}Eu_xTiO_4$ at 300 K. The excitation wavelength is 401.6 nm which is the optimum excitation wavelength for the strongest emission. The emission spectra exhibit two strong lines, which correspond to the $^5D_0$–$^7F_1$ and $^5D_0$–$^7F_2$ transitions of Eu$^{3+}$ [16]. Several weak emissions from higher $^5D$ levels were also observed in the range 400–500 nm for the cases with low concentrations of Eu$^{3+}$ ions.
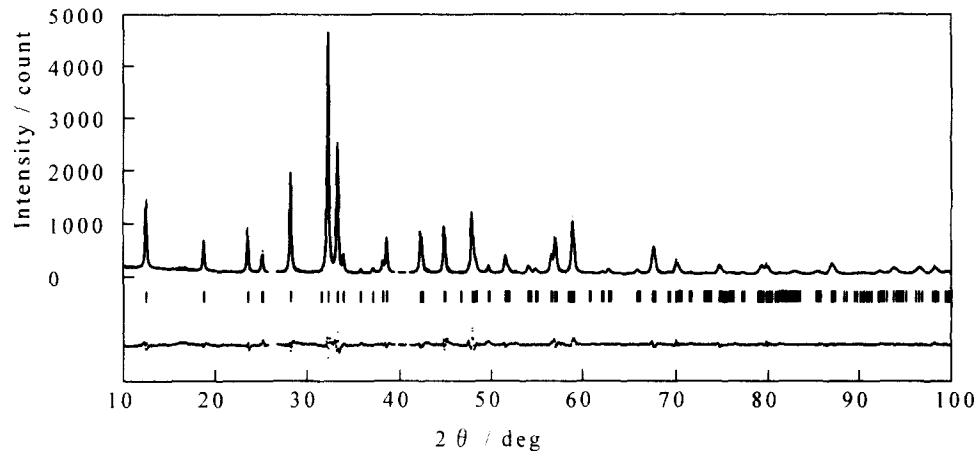
Fig. 1. X-ray powder pattern fitting for $Na_2Eu_2Ti_3O_{10}$. The calculated and observed patterns are shown on the top solid line and the dots. The vertical marks in the middle show positions calculated for Bragg reflections. The trace on the bottom is a plot of the difference between calculated and observed intensities.
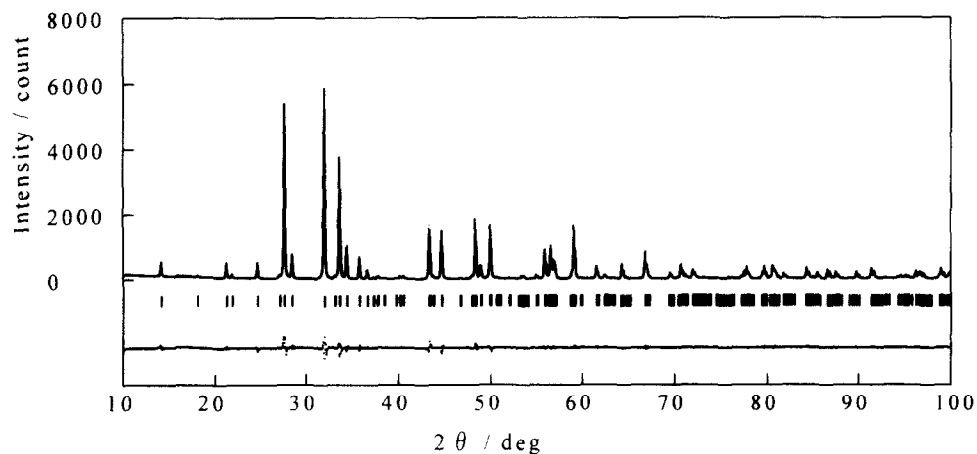


Fig. 2. X-ray powder pattern fitting for $NaEuTiO_4$.

Table 1
Crystallographic data for $Na_2Eu_2Ti_3O_{10}$

| Atom | Site[a] | x | y | z | B (nm²) |
|------|------|-----|-----|-----------|-----------|
| Na | 4e | 0.0 | 0.0 | 0.2882(10) | 0.0004(77) |
| Eu | 4e | 0.0 | 0.0 | 0.4241(2) | 0.012(2) |
| Ti(1) | 2a | 0.0 | 0.0 | 0.0 | 0.005 |
| Ti(2) | 4e | 0.0 | 0.0 | 0.1478(5) | 0.005 |
| O(1) | 4c | 0.0 | 0.5 | 0.0 | 0.11(3) |
| O(2) | 4e | 0.0 | 0.0 | 0.0635(22) | 0.065(20) |
| O(3) | 4e | 0.0 | 0.0 | 0.2076(16) | 0.020(13) |
| O(4) | 8g | 0.0 | 0.5 | 0.1331(12) | 0.025(11) |

| | |
|---|---|
| Space group | $I4/mmm$ |
| Lattice constants (nm) | $a = 0.37956(2)$, $c = 2.8280(1)$ |
| Reliability factors | $R_{wp} = 0.1132$, $R_p = 0.0870$, $R_E = 0.0783$, $R_I = 0.0400$, $R_F = 0.0202$ |

[a] Multiplicity and Wyckoff notation.

Table 2
Crystallographic data for $NaEuTiO_4$

| Atom | Site[a] | x | y | z | B (nm²) |
|------|------|-----------|-----------|------|-----------|
| Na | 4d | 0.9122(9) | 0.0098(37) | 0.25 | 0.0127(26) |
| Eu | 4d | 0.6077(2) | 0.0187(5) | 0.25 | 0.0031(5) |
| Ti(1) | 4d | 0.2334(4) | 0.0051(17) | 0.25 | 0.005 |
| O(1) | 4c | 0.2792(16) | 0.25 | 0.0 | 0.0105(59) |
| O(2) | 4c | 0.7451(17) | 0.25 | 0.0 | 0.005 |
| O(3) | 4d | 0.1002(13) | 0.0362(46) | 0.25 | 0.0033(45) |
| O(4) | 4d | 0.4308(14) | −0.0510(54) | 0.25 | 0.0019(53) |

| | |
|---|---|
| Space group | $Pbcm$ |
| Lattice constants (nm) | $a = 1.25445(2)$, $b = 0.53292(3)$, $c = 0.53279(2)$ |
| Reliability factors | $R_{wp} = 0.1072$, $R_p = 0.0773$, $R_E = 0.0856$, $R_I = 0.0325$, $R_F = 0.0231$ |

[a] Multiplicity and Wyckoff notation.

Fig. 6 shows the dependence of the strongest $^5D_0$–$^7F_2$ emission intensity on the $Eu^{3+}$ concentration. The critical values for the concentration quenching are $x = 0.40$ for $Na_2Gd_{2(1-x)}Eu_{2x}Ti_3O_{10}$ and $x = 0.25$ for

$NaGd_{1-x}Eu_xTiO_4$. The experimental value of the critical concentration for $NaGd_{1-x}Eu_xTiO_4$ is in good agreement with the result of Berdowski and Blasse [4, 17]. Although the $Eu^{3+}$–$Eu^{3+}$ distances in these compounds are rather short, these values are much higher than those observed
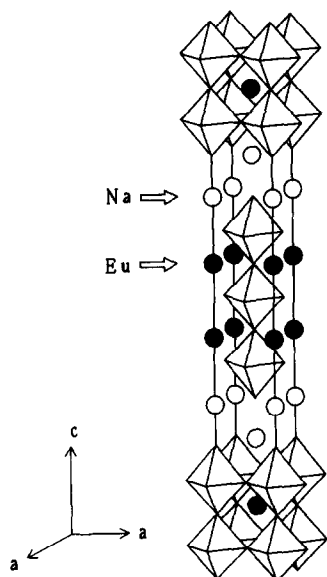
Fig. 3. Structural model of $Na_2Eu_2Ti_3O_{10}$.
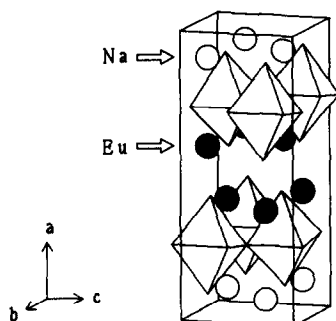


Fig. 4. Structural model of $NaEuTiO_4$.
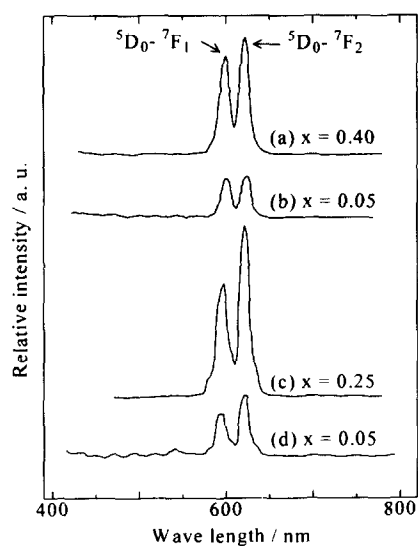


Fig. 5. Emission spectra of $Na_2Gd_{1.2}Eu_{0.8}Ti_3O_{10}$ (spectrum a), $Na_2Gd_{1.9}Eu_{0.1}Ti_3O_{10}$ (spectrum b), $NaGd_{0.75}Eu_{0.25}TiO_4$ (spectrum c) and $NaGd_{0.95}Eu_{0.05}TiO_4$ (spectrum d) at 300 K with 401.6 nm excitation.
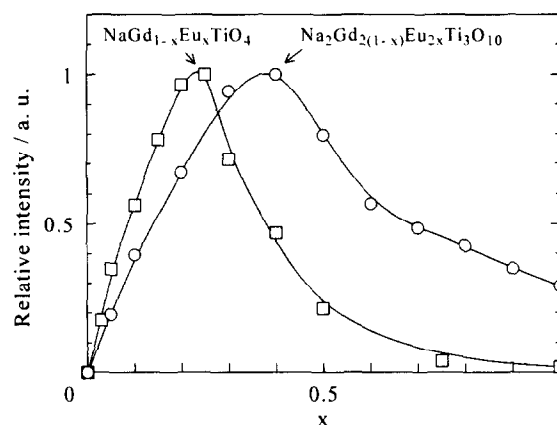


Fig. 6. The dependence of $^5D_0$–$^7F_2$ emission intensity on $Eu^{3+}$ concentration.
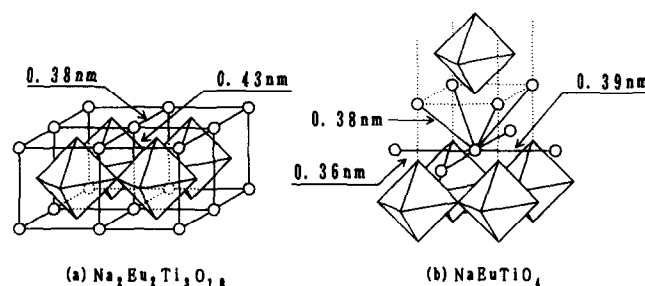


Fig. 7. Schematic representation of local environment of $Eu^{3+}$ ions for $Na_2Eu_2Ti_3O_{10}$ and $NaEuTiO_4$. $Eu^{3+}$ sites and $TiO_6$ octahedra are shown as open circles and octahedra respectively.

in conventional inorganic phosphors [18,19]. The high critical values in the layered perovskite compounds indicate that the energy transfer is restricted to the quasi-two-dimensional $Eu^{3+}$ sublattice.

The theoretical values of the critical concentrations in both compounds were determined by the following approximate expression using the percolation model [20,21], because it is impossible to solve the problem analytically

$$zP_c = d/(d-1) \tag{1}$$

where $z$ is the coordination number, $P_c$ the critical concentration and $d$ the dimensionality for the percolation lattice. It should be noted that this expression gives only an approximate value. Computer simulations are now in progress to obtain more accurate values. The percolation model can be applied to the given compounds based on the following two assumptions: (i) the interaction among $Eu^{3+}$ ions occurs only among the nearest sites; (ii) the concentration quenching is due to the energy transfer from a percolation cluster of the nearly-two-dimensional $Eu^{3+}$ sublattice to killer centres, e.g. unknown defects or a very small amount of impurities acting as an acceptor.

Fig. 7 shows the schematic representation of the local environment of $Eu^{3+}$ ions. There are two kinds of distance among the adjacent $Eu^{3+}$–$Eu^{3+}$ ions in

$Na_2Eu_2Ti_3O_{10}$, i.e. one group is four shortened distances (0.37956(2) nm) and the other a long distance (0.429(1) nm). The distances for the adjacent $Eu^{3+}$ ions for $NaEuTiO_4$ are classified into three types, i.e. two shortened distances (0.3630(4) nm), four moderate distances (0.3795(3) nm, 0.3800(3) nm), and two long distances (0.3911(4) nm). These distances can be considered as nearly equal. Therefore, the coordination numbers $z$ are 5 for $Na_2Gd_{2(1-x)}Eu_{2x}Ti_3O_{10}$ and 8 for $NaGd_{1-x}Eu_xTiO_4$. Since the value of $d$ can be taken as 2 owing to the layered structure, the critical concentration $P_c$ determined by Eq. (1) corresponds to $x = 0.40$ for $Na_2Gd_{2(1-x)}Eu_{2x}Ti_3O_{10}$ and $x = 0.25$ for $NaGd_{1-x}Eu_xTiO_4$. The experimental values agree well with the calculation results. This clearly indicates that the energy transfer occurs only within the nearest $Eu^{3+}$ ions in both compounds.

Berdowski and Blasse [17] claim that the interaction between the $Eu^{3+}$ ions in two-dimensional compounds is due to a superexchange interaction. In this case, the superexchange interaction takes place by spin exchange via the $O^{2-}$ anion. If the nature of the interaction for these compounds is the superexchange, the interaction between the second-nearest-neighbouring $Eu^{3+}$ ions should also become important. The critical concentrations observed are too large on the basis of such a superexchange mechanism only. Since the interaction occurs between the nearest sites, a direct interaction, i.e. multiple–multipole interaction, must be taken into account. Therefore, the interaction between $Eu^{3+}$ ions in the layered perovskite compounds is considered to be due to a multipole–multipole mechanism. Furthermore, such short critical distances of the interaction suggest that the mechanism of higher multipoles (dipole–quadrupole, quadrupole–quadrupole) is dominant in the energy transfer between the $Eu^{3+}$ ions in these compounds. These explanations can satisfactorily interpret the well-known facts that the low-dimensional compounds have a high critical value of concentration quenching.

## References

[1] G. Blasse, J. Alloys Comp., 192 (1993) 17.
[2] L.G. Van Uitert, R.C. Linares, R.R. Soden and A.A. Ballman, J. Chem. Phys., 36 (1962) 702.
[3] L.G. Van Uitert and S. Iida, J. Chem. Phys., 37 (1962) 986.
[4] P.A.M. Berdowski and G. Blasse, J. Lumin., 29 (1984) 243.
[5] F.W. Tian, C. Fouassier and P. Hagenmuller, J. Phys. Chem. Solids, 48 (1987) 245.
[6] T. Endo, A. Shibuya, H. Takizawa and M. Shimada, J. Alloys Comp., 192 (1993) 50.
[7] M. Gondrand and J.-C. Joubert, Rev. Chim. Miner., 24 (1987) 33.
[8] G. Blasse, J. Inorg. Nucl. Chem., 30 (1968) 656.
[9] Y. Takaki, T. Taniguchi, H. Yamaguchi and T. Ogura, J. Ceram. Soc. Jpn., Int. Edn., 95 (1987) 565.
[10] F. Izumi, Nippon Kesshou Gakkaishi, 27 (1985) 23.
[11] D.M. Hatch, H.T. Stokes, K.S. Aleksandrov and S.V. Misyul, Phys. Rev. B, 39 (1989) 9282.
[12] N. Kamegashira, S. Ueno, H. Saito-Nakano and K. Enami, Mater. Res. Bull., 29 (1994) 185.
[13] G. Blasse and G.P.M. Van Den Heuvel, J. Solid State Chem., 10 (1974) 206.
[14] C. Linares and M. Blanchard, C.R. Acad. Sci. Paris Ser. B, 286 (1978) 387.
[15] M.M. Elcombe, E.H. Kisi, K.D. Hawkins, T.J. White, P. Goodman and S. Matheson, Acta Crystallogr. B, 47 (1991) 305.
[16] G. Blasse, in K.A. Gschneidner, Jr., and L. Eyring (eds.), Handbook on the Physics and Chemistry of Rare Earths, North-Holland, Amsterdam, 1979, p. 237.
[17] P.A.M. Berdowski and G. Blasse, J. Solid State Chem., 63 (1986) 86.
[18] A.J. De Vries, J.P.M. Van Vliet and G. Blasse, Phys. Status Solidi B, 149 (1988) 391.
[19] T. Endo, T. Masuda, H. Takizawa and M. Shimada, J. Mater. Sci. Lett., 11 (1992) 1330.
[20] C. Domb and M.F. Sykes, Phys. Rev., 122 (1961) 77.
[21] V.A. Vyssotsky, S.B. Gordon and H.L. Frisch and J.M. Hammersley, Phys. Rev., 123 (1961) 1566.